Space-Time Characterization of the Mobile Radio Channel: an Implementation of the Frequency Sounding Technique

J. F. Macêdo, L. H. Macêdo, R. D. Vieira and G. L. Siqueira
CETUC - PUC/Rio, R. Marquês de São Vicente, 225, Rio de Janeiro - RJ, Brazil, 22453-900, Phone: +55 21 31141694
jfmacedo@cetuc.puc-rio.br; lhmacedo@cetuc.puc-rio.br; robson@cetuc.puc-rio.br; glaucio@cetuc.puc-rio.br

***Abstract*- This work presents the results of an estimation of the mobile radio channel space-time dispersion in 1.8 GHz, through the use of the Frequency Sounding Technique. Some changes in the classical technique were implemented: a set of antennas known as array was built and calibrated, and a processing algorithm of the measured signal was tested. The chosen antennas array is circular with 8 elements. Measured data were taken in a small indoor environment in the campus facility. Results accomplishing for the main propagation mechanisms in the tested scenario are reported, and the technique performance are presented and discussed.**

I. INTRODUCTION

Indoor communications have grown in interest in the past few years. Such growing interest is justified by the imminent beginning of 3rd generation mobile systems operation in some countries, and by the consolidation of some standards (IEEE 802.11 and HyperLAN) that are greatly increasing the wireless LANs use around the world. One of the greatest challenges to such systems deployment is guaranteeing that the high data transmission rates established are reached and sustained. To achieve such high performances, a thorough knowledge of the propagation channel is demanded.

The outdoor and indoor mobile radio propagation channels are usually affected by the presence of a huge amount of scatterers, which give rise to the so-called multi-path effect. In old narrow band communications systems, with only one receiver sensor, is reasonable to know only the power of the received signal and its distribution along the time. However, as the time passed, radio channel models were improved with the addition of delay spread information, which is useful in the optimization of the performance of digital systems [1]. In the field, time dispersion is accomplished by a wide-band sounding; this can be carried out with the classical frequency domain technique implemented with a vector network analyzer (VNA) [2]. Nowadays, with the emerging systems based on multiple sensors arrays, it's necessary to model the signal strength as well as the time and angle of arrival (AOA) of each propagation path. The complete knowledge of these parameters is known as Space-Time Characterization of the Radio Channel.

Attempting to fill partially the needs just mentioned, a research survey has been carried out and the complete set of results is presented in [3]. This paper briefly presents some of the main results of that work, and point to some investigations still under development.

A brief description of the whole survey procedure is presented at section II, including the setup description itself, the modifications in classical VNA technique applied by the use of an array of sensors, and the sounded environment. Section III presents the data processing procedure and the extra signal information obtained with the use of Pointing Matrices. At the following section, the results of the measurement campaign are illustrated and explained. At last, section V includes some concluding remarks regarding this work.

II. SURVEY DESCRIPTION

A. Setup

The setup has two important elements: the Network Analyzer and the antenna array. The VNA sweeps a wild frequency band reporting magnitude and phase data from the Radio Channel. For this, transmission and receiver port are connected to antennae making the local environment the device under test (DUT). To achieve space-time measurements at least one of those sensors should be replaced by an array of antennae, or a synthetic aperture system [4]. In this work we built a circular antenna array, which consists of eight nominally identical quarter wave monopole elements, mounted at a constant radius and separated by one-third wavelength. The signal received at each element is fed to a set of switches, responsible to connect the array with the Analyzer.

The complete setup, sketched in Fig. 1, includes: a HP8714ET VNA, a 2.14 dBi disconical omnidirectional antenna especially built for this band, an eight-element array, a set of switches, a low noise amplifier in the reception, a high-power amplifier, located at the base of the transmit antenna, a 50m run of coaxial cable and a laptop computer for data acquisition and control of both the VNA and switches. The setup calibration has been carried out as the one described in [5], storing in the VNA all the unavoidable effects of the system's components before each measurement, antennas excluded. The mobile unit chosen was the transmitter, in order to keep the Network Analyzer, the computer and the array standstill.

B. Measurements

A 200 MHz band, centered in 1.8 GHz and acquired with 801 samples have been employed to report the amplitude and phase variations of the channel. Measurements have been carried out in a representative scenario in the university campus. The site was a floor of a small office building with narrow corridors; Fig. 2 depicts an in-scale sketch of this corridor. Both line-of-sight (LOS) and out-of-sight (OOS) situations have been assessed.

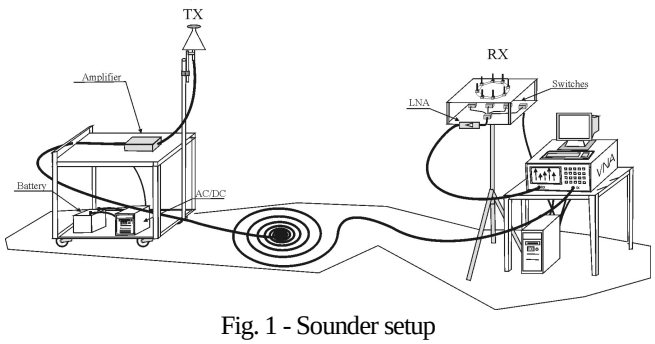

Fig. 1 - Sounder setup

III. SIGNAL PROCESSING

The analysis method employed in this work is based on the minimization of a cost function subject to a constraint [6]. The algorithm is implemented to find a set of optimal weights that, when multiplied by a measurement matrix, generates a vector that gathers its energy principally from determined direction while being insensitive to energy arriving from all other directions.

It's well known that the array structure implemented in this work suffers from high multiple coupling and shadowing between elements. Hence, to find the optimal set of weights, previous knowledge of the signal behavior in certain directions is required in order to consider inherent mismatches of the ensemble.

A. Pointing Matrices

The Pointing Matrices represent the system answer to different directions, giving a priori knowledge of the signal structure, which is provided because the signal is taken to determined direction in the interval 0 to 360° [7].

To create these matrices, the transmit antenna and receiving array were assembled in an anechoic environment separated by a distance of 3 m. This procedure assures that spurious arrivals are very attenuated if compared with the line-of-sight arrival. So, 64 frequency swaps in the eight-elements arragvy are conducted. Between each data set, the array was rotated 5.625° in azimuth, relative to its previous orientation. This measurement and rotation sequence was performed until the complete revolution of the array. In the end of the process, 64 complex matrices, U_m, with 801x8 elements are obtained:

$$U_m = \begin{bmatrix} u_{1,1} & u_{1,2} & \cdots & u_{1,8} \\ u_{2,1} & u_{2,2} & & \\ \vdots & \vdots & \ddots & \\ u_{801,1} & u_{801,2} & & u_{801,8} \end{bmatrix} \quad (1)$$

where m =1,2,3,...,64 corresponds to the directions of the array such that U_1 corresponds to 0°, U_2 corresponds to 5.625°, and so forth.

B. Spatial Filter Algorithm

The analysis tool implemented in this work tries to find the optimal tap weights through the previous knowledge of the signal represented by Pointing Matrices previously discussed.

To find the optimal tap vector w, a cost function is formed, minimizing the array sensitivity to energy from all directions, except the desired [8]:

$$f(w_m) = \sum_{j \neq m}^{801} \sum_{l=1} \left(\sum_{n=1}^{8} u_{l,n,j} \cdot w_{n,m} \right) \left(\sum_{n=1}^{8} u^*_{l,n,j} \cdot w^*_{n,m} \right) \quad (2)$$

where u_{xx} are the elements of the Pointing Matrices and w is the tap weight vector.

The cost function is subject to the additional constraint, which normalizes the signal from the desired direction.

$$c(w_m) = \sum_{l=1}^{801} \left(\sum_{n=1}^{8} u_{l,n,j} \cdot w_{n,m} \right) \left(\sum_{n=1}^{8} u^*_{l,n,j} \cdot w^*_{n,m} \right) - 1 = 0 \quad (3)$$

The method of complex Lagrange multipliers is used to transform the constrained problem in an unconstrained problem. Equations (2) and (3) are combined to form the adjoint equation:

$$\frac{\partial f(w_m)}{\partial w^*_m} + \lambda \frac{\partial c(w_m)}{\partial w^*_m} = 0 \quad (4)$$

Solving (4) leads to a system of eight equations, as follows:

$$F_k(w_m, \lambda) = \sum_{j \neq m}^{801} \sum_{n=1}^{8} u_{l,k,j} \sum_{n=1}^{8} u^*_{l,n,j} \cdot w_{n,m} + \lambda \sum_{l=1}^{801} u^*_{l,k,m} \sum_{n=1}^{8} u^*_{l,k,m} \cdot w_{n,m} = 0 \quad (5)$$

where k =1,2,...,8, corresponds to each element of the vector w.

Taken together, these 8 equations and the constraint, produce a system of nine equations that provides, in the end of the process, the optimal taps for the array processor and the Lagrange multiplier λ. So, the ninth equation is:

$$F_9(w_m, \lambda) = \sum_{l=1}^{801} \left(\sum_{n=1}^{8} u_{l,n,m} \cdot w_{n,m} \right) \left(\sum_{n=1}^{8} u^*_{l,n,m} \cdot w^*_{n,m} \right) - 1 = 0 \quad (6)$$

Newton's iterative method was applied to solve this system of equations. The method is applied 64 times resulting in 64 optimal tap weight vectors with 8 elements each, as shown in equation (7). To each direction a random number of interactions is performed until the weights founded could make the left side of equation (3) less or equal to 10-6. Tests revealed that this stop criterion could guarantee the convergence of the algorithm.

$$W_m = \begin{bmatrix} w_1 & w_2 & \cdots & w_8 \end{bmatrix}^T \quad (7)$$

where m =1,2,3,...,64 corresponds to the directions of the array and T denotes transposition .

After that, an arbitrary measurement matrix V, with 801x8 elements, may be chosen.

$$V = \begin{bmatrix} v_{1,1} & v_{1,2} & \cdots & v_{1,8} \\ v_{2,1} & v_{2,2} & & \\ \vdots & \vdots & \ddots & \\ v_{801,1} & v_{801,2} & & v_{801,8} \end{bmatrix} \quad (8)$$

The multiplication of copies of this matrix by the W vectors results in correspondent columns of the optimal 801x64 matrix X.

$$X = \begin{bmatrix} V \cdot W_1 & V \cdot W_2 & \cdots & V \cdot W_{64} \end{bmatrix} \quad (9)$$

In order to obtain the final spatial-temporal matrix, each column of X is modified with a three terms Blackman Harris window [9]. The final matrix is obtained after inverse Fourier Transform. The result is an 801x64 spatial-temporal matrix $Y(\tau,\theta)$, where the column index indicates the angle of arrival in 5.625° increments, and the row index indicates the time of arrival in 5 ns increments.

$$Y = \begin{bmatrix} y_{1,1} & y_{1,2} & \cdots & y_{1,64} \\ y_{2,1} & y_{2,2} & & \\ \vdots & \vdots & \ddots & \\ y_{801,1} & y_{801,2} & & y_{801,64} \end{bmatrix} \quad (10)$$

IV. RESULTS

Four different measurement results are showed, three in line-of-sight (LOS) and the other in an out-of-sight (OOS) situation.

The first measurement, CETUC1, is in line-of-sight (LOS) situation. The separation transmitter receiver is showed in Fig. 2. Note that there is a metallic locker in the end of the corridor. The marker next to the receptor indicates the reference (0°) of the array. Fig. 3 illustrates a two-dimensional vision of the discrete space-temporal matrix. The magnitudes of the detected rays are presented in a scale of symbols. Fig. 4 gives a 3D visualization of the results. Both figures show spatial sidelobes positioned near the expected signals. These sidelobes are spurious signals and they represent the main limitation of the technique.

Observing the transmitter-receiver positioning in the measurement scenario and the two-dimensional scatter plot of the results lead to the identification of some ray's path. In figure 3, it's visible a direct ray that arrives at 53[ns] from 0° (A) and other ray that arrives at 177 [ns] from 0° (B). The ray (B) is transmitted, propagates until the locker, is reflected and finally arrives at the receiver. According to the separation transmitter-receiver and the position of the principal scatters of the scenario, the rays arrived with expected propagation delays and direction of arrivals.

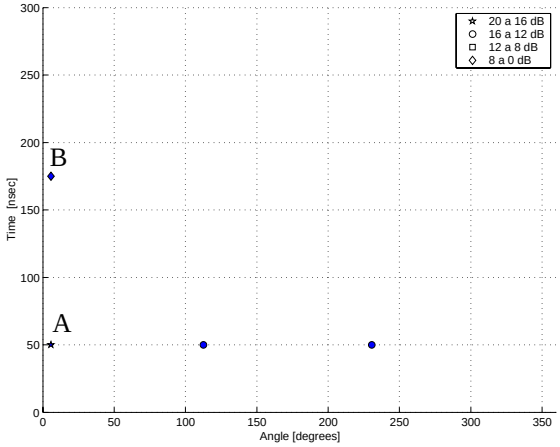

Fig. 3 – CETUC1 results in two-dimensional visualization

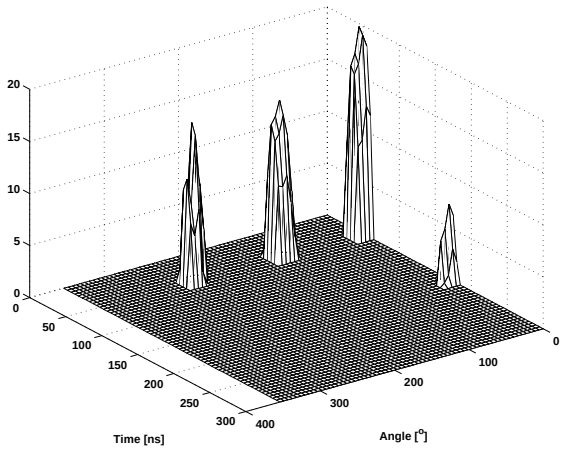

Fig. 4 - CETUC1 results in 3D visualization

Measurement CETUC2, Fig. 5, has the same transmitter-receiver separation that CETUC1, but in CETUC2 a metallic reflector was positioned, behind the receiver, for tests purpose. In Fig. 6, it's possible to recognize three different rays: a direct ray in 0° (A), a ray in 180° (B) and a last ray in 0° (C). The first ray is transmitted and arrives at the receiver directly. The second ray is transmitted, propagates until the metallic reflector and then, arrives at the receiver from 180° at 97 [ns]. This ray was not visible in CETUC1. The last one is transmitted, propagates until the locker, is reflected and finally arrives at the receiver. Note that the propagation delays are coherent with path lengths in all multi-paths.

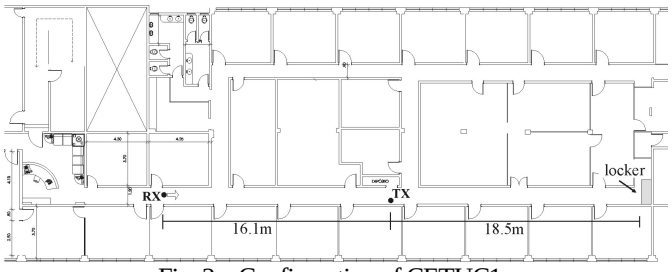

Fig. 2 – Configuration of CETUC1

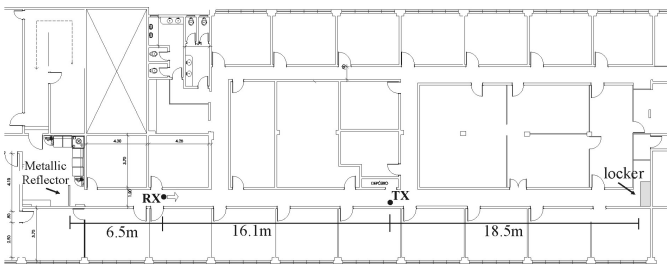

Fig. 5 – Configuration of CETUC2

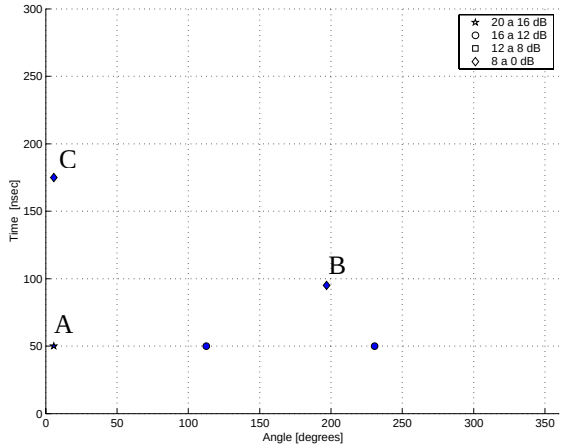

Fig. 6 - CETUC2 results in two-dimensional visualization

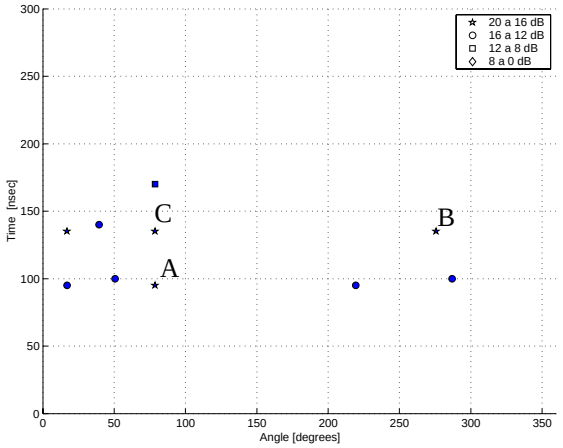

Fig. 9 - CETUC3 results in two-dimensional visualization

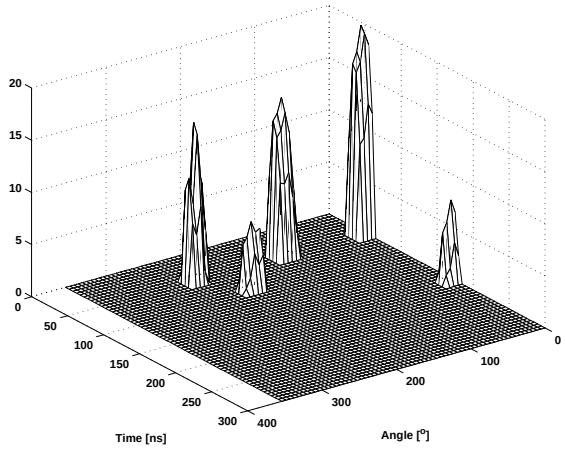

Fig. 7 - CETUC2 results in 3D visualization

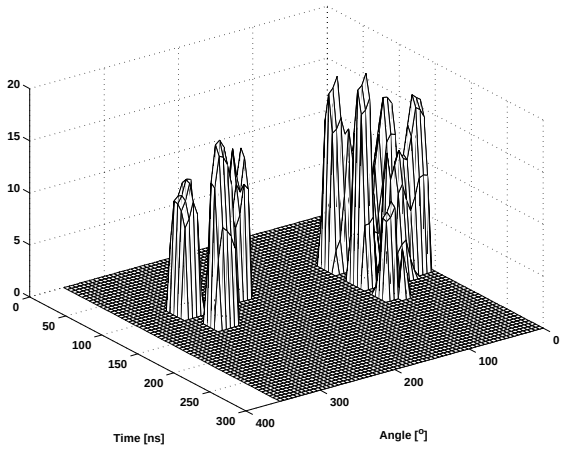

Fig. 10 - CETUC3 results in 3D visualization

Measurement CETUC3 is presented in Fig. 8. In this case, the array's reference is not pointing to the transmitter. So, rays arriving at the receiver from 90^o and 270^o are expected. An analysis similar to the performed in the CETUC2 case can be done. There is a direct ray (A), other reflected by the metallic reflector (B) and the last one reflected by the locker (C). These rays arrive at the receiver with 90^o, 270^o and 90^o, respectively.

The last measurement, CETUC4, is in out-of-sight (OOS) situation. The receptor is positioned in the intersection of two corridors, receiving confined rays from the two directions. The separation transmitter receiver is showed in Fig. 11. Like mentioned, the marker next to the receptor indicates the reference of the array. So, in this measurement, rays with 0^o and 90^o are expected. Even in out-of-sight (OOS) situation, propagation delays are coherent with path lengths.

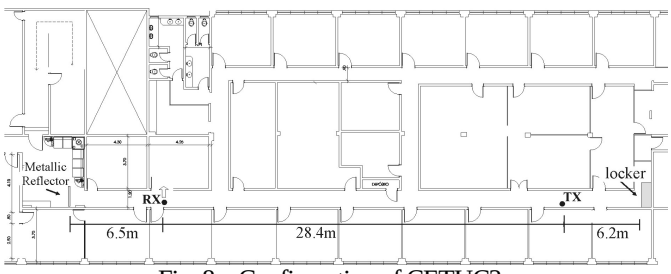

Fig. 8 – Configuration of CETUC3

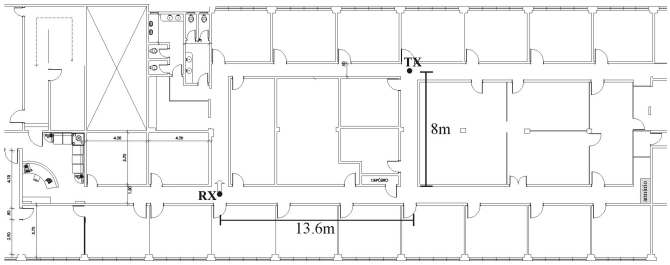

Fig. 11 – Configuration of CETUC4

V. Concluding Remarks

This work presented the results for the spatial-temporal characterization of indoor radio propagation. The frequency sounding technique was implemented and some measurements in 1.8 GHz were taken. Results demonstrate applicability of the measurements methodology adopted. Time delay and direction of arrival were coherent with the position of the principal scatters of the scenario. The measurements illustrated some interesting situations: the guidance of the signal in the measurement CETUC4, and the detection of ray that reaches the receiver with different angles but in the same delay line as depicted in CETUC3.

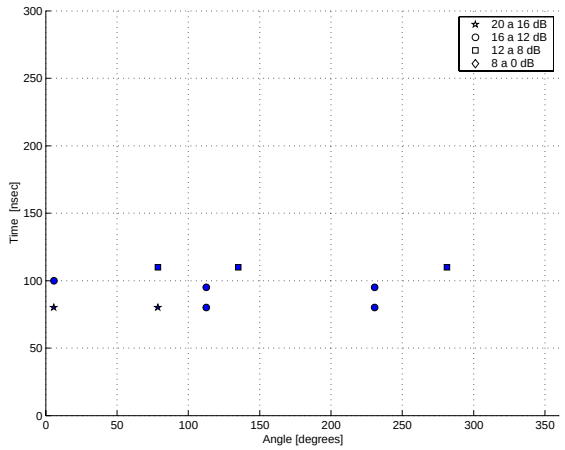

Fig. 12 – CETUC4 results in two-dimensional visualization

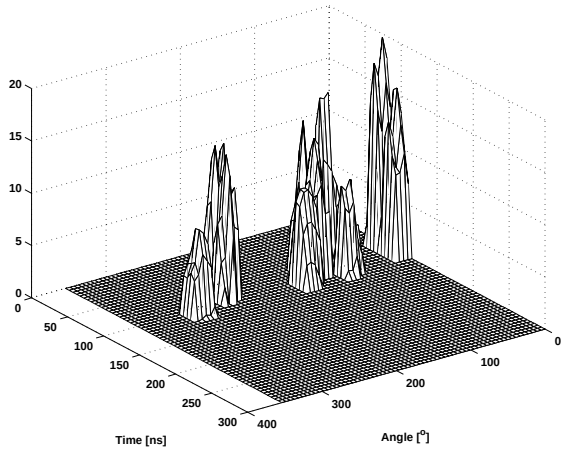

Fig. 13 – CETUC4 results in 3D visualization

ACKNOWLEDGMENT

The authors wish to express their gratitude to Vivian Carvalho for her help during the measurement campaign.

National Counsel for Technological Development – CNPq – Brazil supported this work.

REFERENCES

[1] R. B. Ertel, P. Cardieri, K. Sowerby, T. S. Rappaport "Overview of spatial channel models for antenna array communications systems", *IEEE Personal Communications*, vol. 5, no. 1, pp. 10-22, February 1998.

[2] L. H. Macêdo, R. D. Vieira, J. F. Macêdo, M. H. Dias, G. L. Siqueira, "Mobile indoor wide-band 1.8 GHz sounding: measurement-based time dispersion analysis", *Vehicular Technology Conference*, vol. 1, pp. 375-379, May 2002.

[3] J. F. Macêdo, "Space-time characterization of the mobile radio channel" *(Caracterização espaço-temporal do canal rádio móvel)*, M. Sc. Dissertation (in portuguese), Pontifícia Universidade Católica do Rio de Janeiro, February 2003.

[4] Q. H. Spencer, B. D. Jeffs, A. J. Jensen, A. L. Swindlehurst, "Modeling the statistical time and angle of arrival characteristics of an indoor multipath channel", *IEEE Journal on Selected Areas in Communications*, vol. 18, no. 03, pp. 347-360, March 2000.

[5] S. T. Howard and K. Pahlavan, "Measurement and analysis of the indoor radio channel in frequency domain," *IEEE Transactions of Instrumentation and Measurement*, vol. 39, pp. 751-755, October 1990.

[6] S. Haykin, "Adaptive Filter Theory". Prentice Hall, New Jersey, fourth edition, 2002.

[7] H. Xue, V. Kezys, J. Litva, "Smart antennas calibration for beamforming", *Antennas and Propagation Society International Symposium*, vol. 3, pp. 1458-1461, June 1998.

[8] R. D. Tingley, K. Pahlavan, "Space-Time measurements of indoor radio propagation", *IEEE Transaction on Instrumentation and Measurements*, vol. 50, no. 01, pp. 22-31, February 2001.

[9] F. J. Harris, "On the use of windows for harmonic analysis with the discrete Fourier transform," *IEEE Proceedings*, vol. 66, pp. 51-83, January 1978.